2

Quantum scattering with a spherically symmetric potential

2.1 Introduction

In this chapter, we shall discuss quantum scattering with a spherically symmetric potential as a typical example of the problems studied in computational physics [1, 2]. Scattering experiments are perhaps the most important tool for obtaining detailed information on the structure of matter, in particular the interaction between particles. Examples of scattering techniques include neutron and X-ray scattering for liquids, atoms scattering from crystal surfaces and elementary particle collisions in accelerators. In most of these scattering experiments, a beam of incident particles hits a target which also consists of many particles. The distribution of scattered particles over the different directions is then measured, for different energies of the incident particles. This distribution is the result of many individual scattering events. Quantum mechanics enables us, in principle, to evaluate for an individual event the probabilities for the incident particles to be scattered off in different directions; and this probability is identified with the measured distribution.

Suppose we have an idea of what the potential between the particles involved in the scattering process might look like, for example from quantum mechanical energy calculations (programs for this purpose will be discussed in the next few chapters). We can then *parametrise* the interaction potential, i.e. we write it as an analytic expression involving a set of constants: the parameters. If we evaluate the scattering probability as a function of the scattering angle for different values of these parameters, and compare the results with experimental scattering data, we can find those parameter values for which the agreement between theory and experiment is optimal. Of course, it would be nice if we could evaluate the scattering potential directly from the scattering data (this is called the *inverse problem*), but this is unfortunately very difficult (if not impossible): many different interaction potentials can have similar scattering properties, as we shall see below.

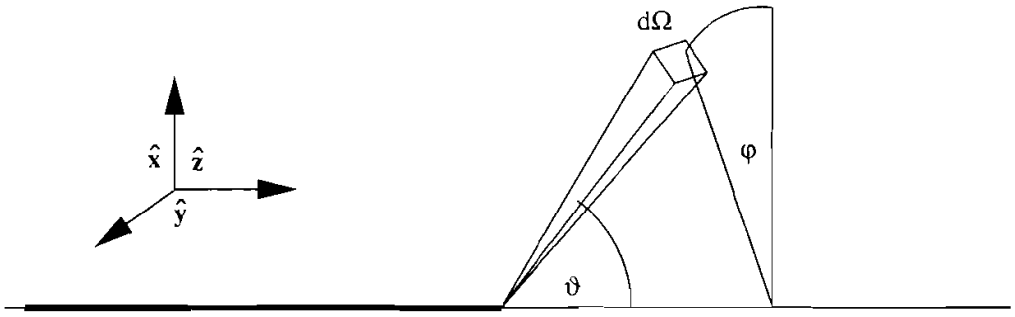

Figure 2.1. Geometry of a scattering process.

There might be many different motives for obtaining accurate interaction potentials. One is that we might use the interaction potential to make predictions about the behaviour of a system consisting of many interacting particles, such as a dense gas or a liquid. Methods for doing this will be discussed in Chapters 8 and 10.

Scattering may be *elastic* or *inelastic*. In the former case the energy is conserved, in the latter it disappears. This means that energy transfer takes place from the scattered particles to degrees of freedom which are not included explicitly in the system (inclusion of these degrees of freedom would cause the energy to be conserved). In this chapter we shall consider elastic scattering. We restrict ourselves furthermore to spherically symmetric interaction potentials. In Chapter 15 we shall briefly discuss scattering in the context of quantum field theory for elementary particles.

We analyse the scattering process of a particle incident on a scattering centre which is usually another particle.[1] We assume that we know the scattering potential, which is spherically symmetric so that it depends on the distance between the particle and the scattering centre only.

In an experiment, one typically measures the scattered flux, that is, the intensity of the outgoing beam for various directions which are denoted by the spatial angle $\Omega = (\theta, \varphi)$ as in Figure 2.1. The *differential cross section*, $\mathrm{d}\sigma(\Omega)/\mathrm{d}\Omega$, describes how these intensities are distributed over the various spatial angles Ω, and the integrated flux of the scattered particles is the *total cross section*, σ_{tot}. These experimental quantities are what we want to calculate.

The scattering process is described by the solutions of the single-particle Schrödinger equation involving the (reduced) mass m, the relative coordinate $\mathbf{r}$ and the interaction potential V between the particle and the interaction centre:

$$\left[-\frac{\hbar^2}{2m}\nabla^2 + V(r)\right]\psi(\mathbf{r}) = E\psi(\mathbf{r}). \tag{2.1}$$

[1] Every two-particle collision can be transformed into a single scattering problem involving the relative position; in the transformed problem the incoming particle has the reduced mass $m = m_1 m_2/(m_1 + m_2)$.

This is a partial differential equation in three dimensions, which could be solved using the 'brute force' discretisation methods presented in Appendix A, but exploiting the spherical symmetry of the potential, we can solve the problem in another, more elegant, way which, moreover, works much faster on a computer. More specifically, in Section 2.3 we shall establish a relation between the *phase shift* and the scattering cross sections. In this section, we shall restrict ourselves to a description of the concept of phase shift and describe how it can be obtained from the solutions of the radial Schrödinger equation. The expressions for the scattering cross sections will then be used to build the computer program which is described in Section 2.2.

For the potential $V(r)$ we make the assumption that it vanishes for r larger than a certain value $r_{\max}$. If we are dealing with an asymptotically decaying potential, we neglect contributions from the potential beyond the range $r_{\max}$, which must be chosen suitably, or treat the tail in a perturbative manner as described in Problem 2.2.

For a spherically symmetric potential, the solution of the Schrödinger equation can always be written as

$$\psi(\mathbf{r}) = \sum_{l=0}^{\infty} \sum_{m=-l}^{l} A_{lm} \frac{u_l(r)}{r} Y_l^m(\theta, \varphi) \tag{2.2}$$

where u_l satisfies the radial Schrödinger equation:

$$\left\{ \frac{\hbar^2}{2m} \frac{\mathrm{d}^2}{\mathrm{d}r^2} + \left[E - V(r) - \frac{\hbar^2 l(l+1)}{2mr^2} \right] \right\} u_l(r) = 0. \tag{2.3}$$

Figure 2.2 shows the solution of the radial Schrödinger equation with $l = 0$ for a square well potential for various well depths – our discussion applies also to nonzero values of l. Outside the well, the solution u_l can be written as a linear combination of the two independent solutions j_l and n_l, the regular and irregular spherical Bessel functions. We write this linear combination in the particular form

$$u_l(r > r_{\max}) \propto kr[\cos\delta_l j_l(kr) - \sin\delta_l n_l(kr)]; \tag{2.4}$$

$$k = \sqrt{2mE}/\hbar.$$

Here $r_{\max}$ is the radius of the well, and δ_l is determined via a matching procedure at the well boundary. The motivation for writing u_l in this form follows from the asymptotic expansion for the spherical Bessel functions:

$$krj_l(kr) \approx \sin(kr - l\pi/2) \tag{2.5a}$$

$$krn_l(kr) \approx -\cos(kr - l\pi/2) \tag{2.5b}$$

which can be used to rewrite (2.4) as

$$u_l(r) \propto \sin(kr - l\pi/2 + \delta_l), \quad \text{large } r. \tag{2.6}$$

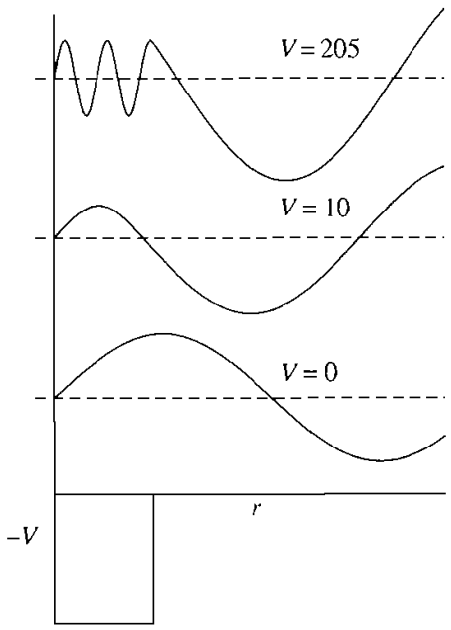

Figure 2.2. The radial wave functions for $l = 0$ for various square well potential depths.

We see that u_l approaches a sine-wave form for large r and the phase of this wave is determined by δ_l, hence the name 'phase shift' for δ_l (for $l = 0$, u_l is a sine wave for all $r > r_{\max}$).

The phase shift as a function of energy and l contains all the information about the scattering properties of the potential. In particular, the phase shift enables us to calculate the scattering cross sections and this will be done in Section 2.3; here we simply quote the results. The differential cross section is given in terms of the phase shift by

$$\frac{\mathrm{d}\sigma}{\mathrm{d}\Omega} = \frac{1}{k^2}\left|\sum_{l=0}^{\infty}(2l+1)\mathrm{e}^{\mathrm{i}\delta_l}\sin(\delta_l)P_l(\cos\theta)\right|^2 \tag{2.7}$$

and for the total cross section we find

$$\sigma_{\mathrm{tol}} = 2\pi\int \mathrm{d}\theta \sin\theta \frac{\mathrm{d}\sigma}{\mathrm{d}\Omega}(\theta) = \frac{4\pi}{k^2}\sum_{l=0}^{\infty}(2l+1)\sin^2\delta_l. \tag{2.8}$$

Summarising the analysis up to this point, we see that the potential determines the phase shift through the solution of the Schrödinger equation for $r < r_{\max}$. The phase shift acts as an intermediate object between the interaction potential and the experimental scattering cross sections, as the latter can be determined from it.

Unfortunately, the expressions (2.7) and (2.8) contain sums over an infinite number of terms – hence they cannot be evaluated on the computer exactly. However, there is a physical argument for cutting off these sums. Classically, only those waves

with an angular momentum smaller than $\hbar l_{\max} = \hbar k r_{\max}$ will 'feel' the potential – particles with higher l-values will pass by unaffected. Therefore we can safely cut off the sums at a somewhat higher value of l; we can always check whether the results obtained change significantly when taking more terms into account. We shall frequently encounter procedures similar to the cutting off described here. It is the art of computational physics to find clever ways to reduce infinite problems to ones which fit into the computer and still provide a reliable description.

How is the phase shift determined in practice? First, the Schrödinger equation must be integrated from $r = 0$ outwards with boundary condition $u_l(r = 0) = 0$. At $r_{\max}$, the numerical solution must be matched to the form (2.4) to fix δ_l. The matching can be done either via the logarithmic derivative or using the value of the numerical solution at two different points r_1 and r_2 beyond $r_{\max}$. We will use the latter method in order to avoid calculating derivatives. From (2.4) it follows directly that the phase shift is given by

$$\tan \delta_l = \frac{K j_l^{(1)} - j_l^{(2)}}{K n_l^{(1)} - n_l^{(2)}} \quad \text{with} \tag{2.9a}$$

$$K = \frac{r_1 u_l^{(2)}}{r_2 u_l^{(1)}}. \tag{2.9b}$$

In this equation, $j_l^{(1)}$ stands for $j_l(kr_1)$ etc.

2.2 A program for calculating cross sections

In this section we describe the construction of a program for calculating cross sections for a particular scattering problem: hydrogen atoms scattered off (much heavier) krypton atoms. Both atoms are considered as single particles and their structure (nucleus and electrons) is not explicitly taken into account. After completion, we are able to compare the results with experimental data. The program described here closely follows the work of Toennies *et al.* who carried out various atomic collisions experimentally and modelled the results using a similar computer program [3].

The program is built up in several steps.

- First, the integration method for solving the radial Schrödinger equation is programmed. Various numerical methods can be used; we consider in particular Numerov's method (see Appendix A7.1).
- Second, we need routines yielding spherical Bessel functions in order to determine the phase shift via the matching procedure Eq. (2.9a). If we want to

calculate differential cross sections, we need Legendre polynomials too. In Appendix A2, iterative methods for evaluating special functions are discussed.

- Finally, we complete the program with a routine for calculating the cross sections from the phase shifts.

2.2.1 Numerov's algorithm for the radial Schrödinger equation

The radial Schrödinger equation is given in Eq. (2.3). We define

$$F(l,r,E) = V(r) + \frac{\hbar^2 l(l+1)}{2mr^2} - E \tag{2.10}$$

so that the radial Schrödinger equation now reads:

$$\frac{\hbar^2}{2m}\frac{\mathrm{d}^2}{\mathrm{d}r^2}u(r) = F(l,r,E)u(r). \tag{2.11}$$

Units are chosen in which $\hbar^2/(2m)$ assumes a reasonable value, that is, not extremely large and not extremely small (see below). You can choose a library routine for integrating this equation but if you prefer to write one yourself, Numerov's method is a good choice because it combines the simplicity of a regular mesh with good efficiency. The Runge–Kutta method can be used if you want to have the freedom of varying the integration step when the potential changes rapidly (see Problem 2.1).

Numerov's algorithm is described in Appendix A7.1. It makes use of the special structure of this equation to solve it with an error of order h^6 (h is the discretisation interval) using only a three-point method. For $\hbar^2/2m \equiv 1$ it reads:

$$w(r+h) = 2w(r) - w(r-h) + h^2 F(l,r,E)u(r) \tag{2.12}$$

and

$$u(r) = \left[1 - \frac{h^2}{12}F(l,r,E)\right]^{-1} w(r). \tag{2.13}$$

It is useful to keep several things in mind when coding this algorithm.

- The function $F(l,r,E)$, consisting of the energy, potential and centrifugal barrier, given in Eq. (2.10), is coded into a function `F(L,R,E)`, with `L` an integer and `R` and `E` being real variables.
- As you can see from Eq. (2.9a), the value of the wave function is needed for two values of the radial coordinate r, both beyond $r_{\max}$. We can take r_1 equal to the first integration point beyond $r_{\max}$ (if the grid constant h for the integration fits an integer number of times into $r_{\max}$, it is natural to take $r_1 = r_{\max}$). The value of r_2 is larger than r_1 and it is advisable to take it roughly half a wavelength beyond the latter. The wavelength is given by $\lambda = 2\pi/k = 2\pi\hbar/\sqrt{2mE}$. As

both r_1 and r_2 are equal to an integer times the integration step h (they will in general not differ by exactly half a wavelength) the precise values of r_1 and r_2 are determined in the routine and output to the appropriate routine parameters.

- The starting value at $r = 0$ is given by $u(r = 0) = 0$. We do not know the value of the derivative, which determines the normalisation of the resulting function – this normalisation can be determined afterward. We take $u_l(0) = 0$ and $u_l(h) = h^{l+1}$ (h is the integration step), which is the asymptotic approximation for u_l near the origin for a *regular* potential (for the H–Kr interaction potential which diverges strongly near the origin, we must use a different boundary condition as we shall see below).

PROGRAMMING EXERCISE

Write a code for the Numerov algorithm. The input parameters to the routine must include the integration step h, the radial quantum number l, the energy E and the radial coordinate $r_{\max}$; on output it yields the coordinates r_1 and r_2 and the values of the wave function $u_l(r_1)$ and $u_l(r_2)$.

When building a program of some complexity, it is very important to build it up step by step and to check every routine extensively. Comparison with analytical solutions is then of prime importance. We now describe several checks that should be performed after completion of the Numerov routine (it is also sensible to test a library routine).

Check 1 The numerical solutions can be compared with analytical solutions for the case of the three-dimensional harmonic oscillator. Bound states occur for energies $E = \hbar\omega(n + 3/2), n = 0, 1, 2, \ldots$ It is convenient in this case to choose units such that $\hbar^2/2m = 1$. Taking $V(r) = r^2$, we have $\hbar\omega = 2$ and the lowest state occurs for $l = 0$ with energy $E = 3.0$, with eigenfunction $Ar\exp(-r^2/2)$, A being some constant. Using $E = 3.0$ in our numerical integration routine should give us this solution with $A = \exp(h^2/2)$ for the starting conditions described above. Check this for r-values up to r_2.

Check 2 The integration method has an error of $\mathcal{O}(h^6)$ (where $\mathcal{O}$ indicates 'order'). The error found at the end of a finite interval then turns out to be less than $\mathcal{O}(h^4)$ (see Problem A3). This can be checked by comparing the numerical solution for the harmonic oscillator with the exact one. Carry out this comparison for several values of N, for example $N = 4, 8, 16, \ldots$ For N large enough, the difference between the exact and the numerical solution should decrease for each new value of N by a factor of at least 16. If your program does not yield this behaviour, there must be an error in the code!

We shall now turn to the H–Kr interaction. The two-atom interaction potential for atoms is often modelled by the so-called Lennard–Jones (LJ) potential, which has the following form:

$$V_{\mathrm{LJ}}(r) = \varepsilon\left[\left(\frac{\rho}{r}\right)^{12} - 2\left(\frac{\rho}{r}\right)^{6}\right]. \tag{2.14}$$

This form of potential contains two parameters, ε and ρ, and for H–Kr the best values for these are

$$\varepsilon = 5.9\,\mathrm{meV} \quad \text{and} \quad \rho = 3.57\,\text{Å}. \tag{2.15}$$

Note that the energies are given in *milli*-electronvolts! In units of meV and ρ for energy and distance respectively, the factor $2m/\hbar^2$ is equal to about $6.12\,\mathrm{meV}^{-1}\rho^{-2}$. The potential used by Toennies *et al.* [3] included small corrections to the Lennard–Jones shape.

For the Lennard–Jones potential the integration of the radial Schrödinger equation gives problems for small r because of the $1/r^{12}$ divergence at the origin. We avoid integrating in this region and start at a nonzero radius $r_{\min}$ where we use the analytic approximation of the solution for small r to find the starting values of the numerical solution. For $r < r_{\min}$, the term $1/r^{12}$ dominates the other terms in the potential and the energy, so that the Schrödinger equation reduces to

$$\frac{\mathrm{d}^2u}{\mathrm{d}r^2} = \varepsilon\alpha\frac{1}{r^{12}}u(r) \tag{2.16}$$

with $\alpha = 6.12$. The solution of this equation is given by

$$u(r) = \exp(-Cr^{-5}) \tag{2.17}$$

with $C = \sqrt{\varepsilon\alpha/25}$. This fixes the starting values of the numerical solution at $r_{\min}$ which should be chosen such that it can safely be assumed that the $1/r^{12}$ dominates the remaining terms in the potential; typical values for the starting value of r lie between 0.5ρ and 0.8ρ (the minimum of the Lennard–Jones potential is found at $r = 2$). Note that Eq. (2.17) provides the starting value and derivative of the wavefunction u at the starting point. In Appendix A7.1 a procedure is described by which two consecutive values can then be found which, when used as the starting values of the Numerov method, provide a solution with the proper accuracy. This will not be the case when two consecutive points are simply set to the solution Eq. (2.17), as this is not an exact solution to either the continuum differential equation or to its discrete (Numerov) form.

You can adapt your program to the problem at hand by simply changing the function $F(l, r, E)$ to contain the Lennard–Jones potential and by implementing the boundary conditions as described. As a check, you can verify that the solution does not become enormously large or remain very small.

2.2.2 The spherical Bessel functions

For the present problem, you need only the first six spherical Bessel functions j_l and n_l, and you can type in the explicit expressions directly. If you want a general routine for the spherical Bessel functions, however, you can use the recursive procedures described in Appendix A (see also Problem A1). Although upward recursion can be unstable for j_l (see Appendix A), this is not noticeable for the small l values (up to $l = 6$) that we need and you can safely use the simple upward recursion for *both* n_l and j_l (or use a library routine).

PROGRAMMING EXERCISE

Write routines for generating the values of the spherical Bessel functions j_l and n_l. On input, the values of l and the argument x are specified and on output the value of the appropriate Bessel function is obtained.

Check 3 If your program is correct, it should yield the values for j_5 and n_5 given in Problem A1.

2.2.3 Putting the pieces together: results

To obtain the scattering cross sections, some extra routines must be added to the program. First of all, the phase shift must be extracted from the values r_1, $u(r_1)$ and r_2, $u(r_2)$. This is straightforward using Eq. (2.9a). The total cross section can then readily be calculated using Eq. (2.8). The choice of $r_{\max}$ must be made carefully, preferably keeping the error of the same order as the $\mathcal{O}(h^6)$ error of the Numerov routine (or the error of your library routine). In Problem 2.2 it is shown that the deviation in the phase shift caused by cutting off the potential at $r_{\max}$ is given by

$$\Delta\delta_l = -\frac{2m}{\hbar^2}k\int_{r_{\max}}^{\infty} j_l^2(kr)V_{\mathrm{LJ}}(r)r^2\mathrm{d}r \tag{2.18}$$

and this formula can be used to estimate the resulting error in the phase shift or to improve the value found for it with a potential cut-off beyond $r_{\max}$. A good value is $r_{\max} \approx 5\rho$.

For the determination of the differential cross section you will need additional routines for the Legendre polynomials.[2] In the following we shall only describe results for the total cross section.

PROGRAMMING EXERCISE

Add the necessary routines to the ones you have written so far and combine them into a program for calculating the total cross section.

[2] These can be generated using the recursion relation $(l+1)P_{l+1}(x) = (2l+1)xP_l(x) - lP_{l-1}(x)$.

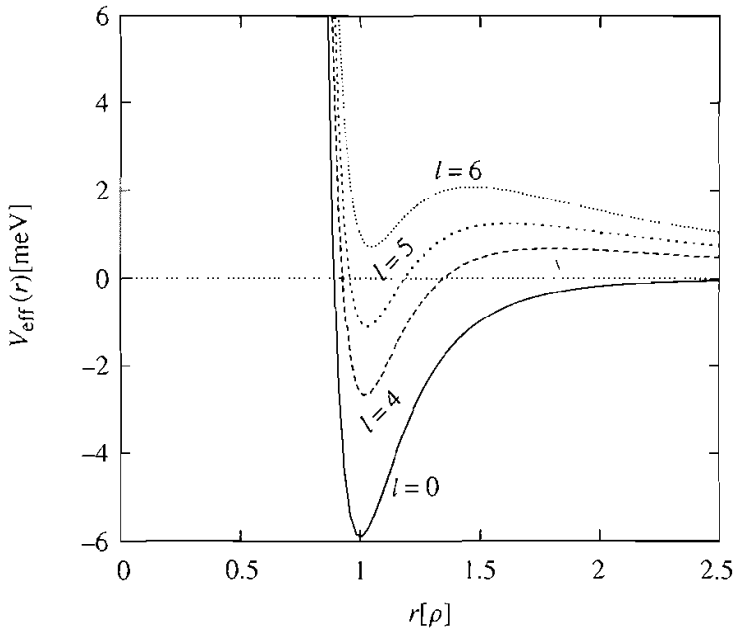

Figure 2.3. The effective potential for the Lennard–Jones interaction for various l-values.

A computer program similar to the one described here was used by Toennies *et al.* [3] to compare the results of scattering experiments with theory. The experiment consisted of the bombardment of krypton atoms with hydrogen atoms. Figure 2.3 shows the Lennard–Jones interaction potential plus the centrifugal barrier $l(l+1)/r^2$ of the radial Schrödinger equation. For higher l-values, the potential consists essentially of a hard core, a well and a barrier which is caused by the $1/r^2$ centrifugal term in the Schrödinger equation. In such a potential, quasi-bound states are possible. These are states which would be genuine bound states for a potential for which the barrier does not drop to zero for larger values of r, but remains at its maximum height. You can imagine the following to happen when a particle is injected into the potential at precisely this energy: it tunnels through the barrier, remains in the well for a relatively long time, and then tunnels outward through the barrier in an arbitrary direction because it has 'forgotten' its original direction. In wave-like terms, the particle resonates in the well, and this state decays after a relatively long time. This phenomenon is called 'scattering resonance'. This means that particles injected at this energy are strongly scattered and this shows up as a peak in the total cross section.

Such peaks can be seen in Figure 2.4, which shows the total cross section as a function of the energy calculated with a program as described above. The peaks are due to $l = 4$, $l = 5$ and $l = 6$ scattering, with energies increasing with l. Figure 2.5 finally shows the experimental results for the total cross section for H–Kr. We see that the agreement is excellent.

You should be able now to reproduce the data of Figure 2.4 with your program.

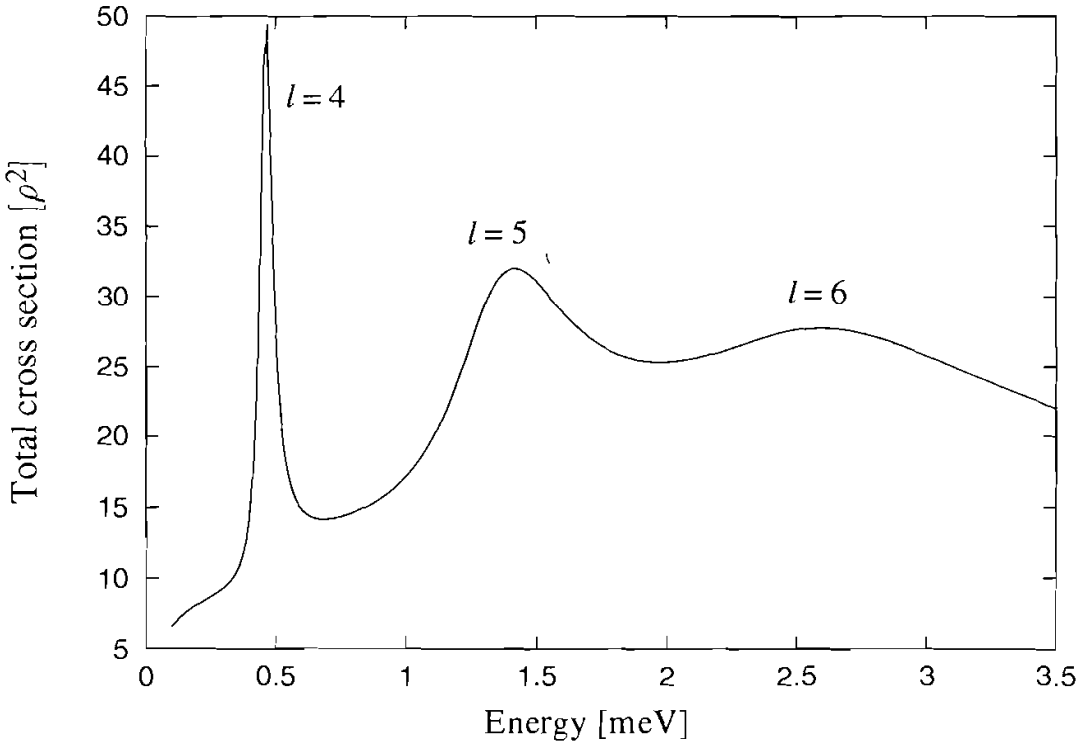

Figure 2.4. The total cross section shown as function of the energy for a Lennard–Jones potential modelling the H–Kr system. Peaks correspond to the resonant scattering states. The total cross section is expressed in terms of the range ρ of the Lennard–Jones potential.

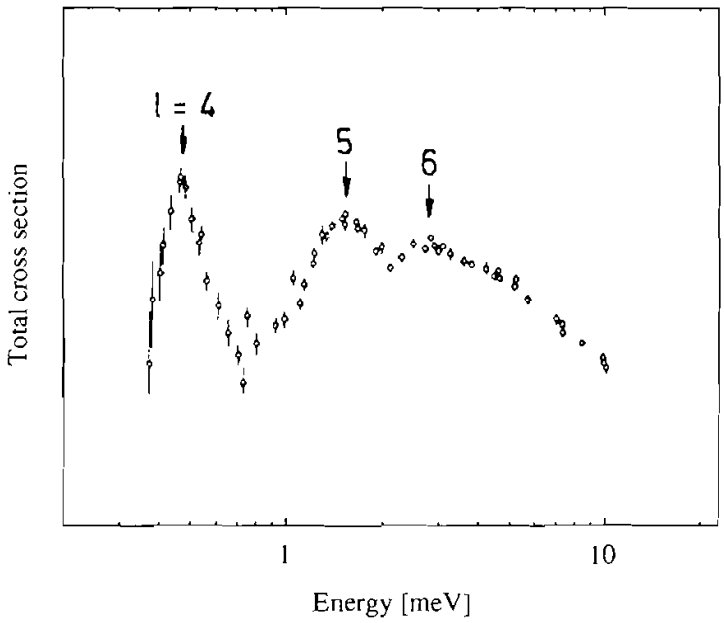

Figure 2.5. Experimental results as obtained by Toennies *et al.* [3] for the total cross section (arbitrary units) of the scattering of hydrogen atoms by krypton atoms as function of centre of mass energy.

*2.3 Calculation of scattering cross sections

In this section we derive Eqs. (2.7) and (2.8). At a large distance from the scattering centre we can make an *Ansatz* for the wave function. This consists of the incoming beam and a scattered wave:

$$\psi(\mathbf{r}) \propto e^{i\mathbf{k}\cdot\mathbf{r}} + f(\theta)\frac{e^{ikr}}{r}. \tag{2.19}$$

Here, θ is the angle between the incoming beam and the line passing through $\mathbf{r}$ and the scattering centre. The function f does not depend on the azimuthal angle φ because the incoming wave has azimuthal symmetry, and the spherically symmetric potential will not generate $m \neq 0$ contributions to the scattered wave. $f(\theta)$ is called the scattering amplitude. From the *Ansatz* it follows that the differential cross section is given directly by the square of this amplitude:

$$\frac{d\sigma}{d\Omega} = |f(\theta)|^2 \tag{2.20}$$

with the appropriate normalisation (see for example Ref. [1]).

Beyond r_{max}, the solution can also be written in the form (2.2) leaving out all $m \neq 0$ contributions because of the azimuthal symmetry:

$$\psi(\mathbf{r}) = \sum_{l=0}^{\infty} A_l \frac{u_l(r)}{r} P_l(\cos\theta) \tag{2.21}$$

where we have used the fact that $Y_0^l(\theta, \phi)$ is proportional to $P_l(\cos\theta)$. Because the potential vanishes in the region $r > r_{max}$, the solution $u_l(r)/r$ is given by the linear combination of the regular and irregular spherical Bessel functions, and as we have seen this reduces for large r to

$$u_l(r) \approx \sin\left(kr - \frac{l\pi}{2} + \delta_l\right). \tag{2.22}$$

We want to derive the scattering amplitude $f(\theta)$ by equating the expressions (2.19) and (2.21) for the wave function. For large r we obtain, using (2.22):

$$\sum_{l=0}^{\infty} A_l \left[\frac{\sin(kr - l\pi/2 + \delta_l)}{kr}\right] P_l(\cos\theta) = e^{i\mathbf{k}\cdot\mathbf{r}} + f(\theta)\frac{e^{ikr}}{r}. \tag{2.23}$$

We write the right hand side of this equation as an expansion similar to that in the left hand side, using the following expression for a plane wave [4]

$$e^{i\mathbf{k}\cdot\mathbf{r}} = \sum_{l=0}^{\infty} (2l+1) i^l j_l(kr) P_l(\cos\theta). \tag{2.24}$$

$f(\theta)$ can also be written as an expansion in Legendre polynomials:

$$f(\theta) = \sum_{l=0}^{\infty} f_l P_l(\cos\theta), \tag{2.25}$$

so that we obtain:

$$\sum_{l=0}^{\infty} A_l \left[\frac{\sin(kr - l\pi/2 + \delta_l)}{kr}\right] P_l(\cos\theta)$$
$$= \sum_{l=0}^{\infty} \left[(2l+1)i^l j_l(kr) + f_l \frac{e^{ikr}}{r}\right] P_l(\cos\theta). \tag{2.26}$$

If we substitute the asymptotic form (2.5a) of j_l in the right hand side, we find:

$$\sum_{l=0}^{\infty} A_l \left[\frac{\sin(kr - l\pi/2 + \delta_l)}{kr}\right] P_l(\cos\theta)$$
$$= \frac{1}{r}\sum_{l=0}^{\infty} \left[\frac{2l+1}{2ik}(-)^{l+1} e^{-ikr} + \left(f_l + \frac{2l+1}{2ik}\right) e^{ikr}\right] P_l(\cos\theta). \tag{2.27}$$

Both the left and the right hand sides of (2.27) contain incoming and outgoing spherical waves (the occurrence of incoming spherical waves does not violate causality: they arise from the incoming plane wave). For each l, the prefactors of the incoming and outgoing waves should be equal on both sides in (2.27). This condition leads to

$$A_l = (2l+1)e^{i\delta_l} i^l \tag{2.28}$$

and

$$f_l = \frac{2l+1}{k} e^{i\delta_l} \sin(\delta_l). \tag{2.29}$$

Using (2.20), (2.25), and (2.29), we can write down an expression for the differential cross section in terms of the phase shifts δ_l:

$$\frac{d\sigma}{d\Omega} = \frac{1}{k^2}\left|\sum_{l=0}^{\infty}(2l+1)e^{i\delta_l}\sin(\delta_l)P_l(\cos\theta)\right|^2. \tag{2.30}$$

For the total cross section we find, using the orthonormality relations of the Legendre polynomials:

$$\sigma_{\text{tot}} = 2\pi \int d\theta \sin\theta \frac{d\sigma}{d\Omega}(\theta) = \frac{4\pi}{k^2}\sum_{l=0}^{\infty}(2l+1)\sin^2\delta_l. \tag{2.31}$$

Exercises

2.1 [C] Try using the Runge–Kutta method with an adaptive time step to integrate the radial Schrödinger equation in the program of Section 2.2, keeping the estimated error fixed as described in Appendix A7.1. What is the advantage of this method over Numerov's method for this particular case?

2.2 [C] Consider two radial potentials V_1 and V_2 and the solutions $u_l^{(1)}$ and $u_l^{(2)}$ to the radial Schrödinger equation for these two potentials (at the same energy):

$$\left[\frac{\hbar^2}{2m}\frac{\mathrm{d}^2}{\mathrm{d}r^2} + \left(E - V_1(r) - \frac{\hbar^2 l(l+1)}{2mr^2}\right)\right] u_l^{(1)}(r) = 0$$

$$\left[\frac{\hbar^2}{2m}\frac{\mathrm{d}^2}{\mathrm{d}r^2} + \left(E - V_2(r) - \frac{\hbar^2 l(l+1)}{2mr^2}\right)\right] u_l^{(2)}(r) = 0.$$

(a) Show that by multiplying the first equation from the left by $u_l^{(2)}(r)$ and the second one from the left by $u_l^{(1)}(r)$ and then subtracting, it follows that:

$$\int_0^L \mathrm{d}r u_l^{(2)}(r)[V_1(r) - V_2(r)]u_l^{(1)}(r) = \frac{\hbar^2}{2m}\left[u_l^{(2)}(L)\frac{\partial u_l^{(1)}(L)}{\partial r} - u_l^{(1)}(L)\frac{\partial u_l^{(2)}(L)}{\partial r}\right].$$

(b) If $V_i \to 0$ for large r, then both solutions are given for large r by $\sin[kr - (l\pi/2) + \delta_l^{(i)}]/k$. Show that from this it follows that:

$$\int_0^\infty \mathrm{d}r u_l^{(2)}(r)[V_1(r) - V_2(r)]u_l^{(1)}(r) = \frac{\hbar^2}{2mk}\sin(\delta_l^{(2)} - \delta_l^{(1)}).$$

Now take $V_1 \equiv 0$ and $V_2 \equiv V$ small everywhere. In that case, $u_l^{(1)}$ and $u_l^{(2)}$ on the left hand side can both be approximated by $rj_l(kr)$, so that we obtain:

$$\delta_l \approx -\frac{2mk}{\hbar^2}\int_0^\infty \mathrm{d}r\, r^2 j_l^2(kr)V(r).$$

This is the *Born approximation* for the phase shift. This approximation works well for potentials that are small with respect to the energy.

(c) [C] Write a (very simple) routine for calculating this integral (or use a library routine). Of course, it is sufficient to carry out the integration up to $r_{\max}$ since beyond that range $V \equiv 0$. Compare the Born approximation with the solution of the program developed in the previous problem. For the potential, take a weak Gaussian well:

$$V(r) = -A\exp[-(r-1)^2], \quad x < r_{\max}$$

and

$$V(r) = 0, \quad x \geq r_{\max}.$$

with $A = 0.01$ and $r_{\max}$ chosen suitably. Result?

(d) Now consider the analysis of items (a) and (b) where V_1 is the Lennard–Jones potential without cut-off and V_2 with cut-off. Show that the phase shift for the

Lennard–Jones potential without cut-off is given by the phase shift for the potential with cut-off plus a correction given by:

$$\Delta\delta_l = \frac{2m}{\hbar^2} k \int_{r_{\max}}^{\infty} j_l^2(kr) V_{\mathrm{LJ}}(r) r^2 \mathrm{d}r.$$

References

[1] A. Messiah, *Quantum Mechanics*, vols. 1 and 2. Amsterdam, North-Holland, 1961.

[2] S. E. Koonin, *Computational Physics*. Reading, Benjamin/Cummings, 1986.

[3] J. P. Toennies, W. Welz, and G. Wolf, 'Molecular beam scattering studies of orbiting resonances and the determination of Van der Waals potentials for H–He, Ar, Kr, and Xe and for H_2–Ar, Kr and Xe,' *J. Chem. Phys.*, **71** (1979), 614–42.

[4] M. Abramowitz and I. A. Stegun, *Handbook of Mathematical Functions*. Washington DC, National Bureau of Standards, 1964.